

On the developments of spectral wave models: numerics and parameterizations for the coastal ocean

Aron Roland¹, Fabrice Ardhuin² *

¹ Institut für Wasserbau und Wasserwirtschaft, Technische Universität Darmstadt, Darmstadt, Germany

² Laboratoire d'Océanographie Spatiale, Ifremer, Plouzan, France

*: Corresponding author : Fabrice Ardhuin, email address : ardhuin@ifremer.fr

Abstract:

The development of numerical wave models for coastal applications, including coupling with ocean circulation models, has spurred an ongoing effort on theoretical foundations, numerical techniques, and physical parameterizations. Some important aspects of this effort are reviewed here, and results are shown in the case of the French Atlantic and Channel coast using version 4.18 of the WAVEWATCH III^R model. Compared to previous results, the model errors have been strongly reduced thanks to, among other things, the introduction of currents, coastal reflection, and bottom sediment types. This last item is described here for the first time, allowing unprecedented accuracy at some sites along the French Atlantic Coast. The adequate resolution, necessary to represent strong gradients in tidal currents, was made possible by the efficiency brought by unstructured grids. A further increase in resolution, necessary to resolve surf zones and still cover vast regions, will require further developments in numerical methods.

Keywords: Wave modeling ; Bottom friction ; Coupling ; Wave-current interaction

1 Introduction

The first spectral numerical wave model was developed in the 1950s to deal with dispersive swell propagation arriving in Morocco. This approach was soon generalized and led to the development of a succession of numerical wave models (SWAMP Group 1984; Komen et al. 1994). So what does it take to make an accurate wave model, and how accurate can be the wave hindcasts in coastal waters? Seven years after the publication of a collective review on numerical wave modeling (WISE Group 2007), the present paper aims at providing some updates on specific issues, in particular, numerical methods and bottom friction. In adapting our

1 paper from the Coastal Dynamics conference (Ardhuin and Roland, 2013) we have
2 left out theoretical aspects related to wave-current interactions, and corrected a
3 few errors.

4 We focus here on numerical wave models in section 2, with an application to the
5 French coast in section 3, followed by perspectives, outlined in section 4. Driven by
6 this application, the present paper is not a full review of a very extensive literature,
7 nor a specific study of a single particular problem. Instead, it touches on several
8 practical issues and attempts to link them to more fundamental problems. Our
9 point of view is centred on the WAVEWATCH III modelling framework (Tolman,
10 2009), and more specifically its application with triangle-based meshes. Still, many
11 aspects discussed below are also relevant to other numerical wave models.
12

13 **2 Spectral wave models: inherent limitations and recent progress**

14 **2.1 Waves, statistics, and spectra**

15 The basic idea of spectral wave modelling is to represent the random nature
16 of the sea surface elevation by its generalized Fourier spectrum, evolving slowly
17 in space and time (Priestley, 1965). Some available spectral models include the
18 phase information, which provides information on wave asymmetry and skewness
19 (Herbers and Burton, 1997, a part of the U.S. Nearshore Community models).
20 This information is particularly relevant in shallow water, but these models have
21 not been widely adopted by the research or engineering community, probably be-
22 cause of the conceptual difficulty of working with both spectra and bi-spectra.
23 Outside of the surf zone, phase-resolving models have been used very successfully
24 in ocean engineering applications, when the details of the wave shape and flow
25 are required (e.g. Dommermuth and Yue, 1987), and also to verify the underlying
26 hypotheses of phase-averaged model and their statistical closure (Tanaka, 2001).
27

28 However, in this region of the ocean, it was found repeatedly by Tayfun (1980)
29 and Fedele and Tayfun (2007) that the full statistics of the sea surface are very
30 well described by the quasi-linear random wave model: waves can be represented
31 as a superposition of wave trains that are locally sinusoidal and that propagate
32 in all possible directions with all possible frequencies, with an intrinsic period
33 $T = 1/f = 2\pi/\sigma$ and wavelength $L = 2\pi/k$ related by the linear dispersion
34 relation for free surface gravity waves $\sigma^2 = gk \tanh(kD)$ as a function of the
35 local mean water depth D (de Laplace, 1776). The intrinsic frequency f is the
36 frequency of waves in the frame of reference moving with the local horizontal
37 “current”. As a result, the general three-dimensional wave spectrum collapses to
38 a two-dimensional spectrum and the phases are essentially random and do not
39 require any particular attention. One only needs to focus on one scalar, the spectral
40 density of sea surface elevation (usually called energy). This scalar is a function of
41 two spectral dimensions that is usually chosen among the pairs wavenumber and
42 direction (k, θ) , frequency and alongshore wavenumber (f, k_y) , or more usually,
43 intrinsic frequency f and direction towards which waves are propagating, θ , as
44 shown in figure 1. From this surface elevation spectrum, it is possible to compute
45 the spectra, and thus the full statistics, of any other wave-related parameter such
46 as velocities, pressure, surface slopes.
47
48
49
50
51
52
53
54
55
56
57
58
59
60
61
62
63
64
65

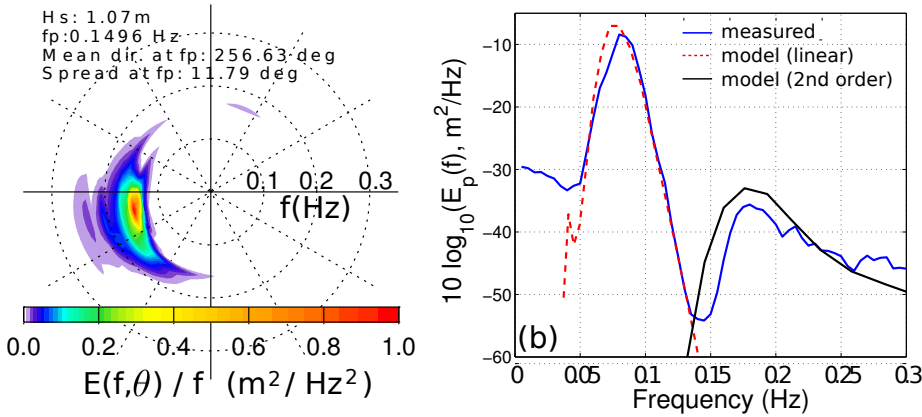


Fig. 1 Two examples of wave spectra. (a) Obtained from a stereo-video system measuring maps of sea surface elevation (Benetazzo, 2006) deployed on the Katsiveli platform near Sevastopol, Ukraine, (b) Spectrum of bottom pressure from a SBE26 tide gauge deployed in 100 m depth offshore of Brest, compared to its simulation from global wind fields using the WW3 code. The measured spectrum is compared to a numerical model result for both the linear part and the second-order correction (Ardhuin et al, 2013). In this case, this second order contribution is the reason why it is impossible to estimate the spectrum for waves with frequencies above 0.13 Hz.

For extreme events, including the famous 'freak waves', a second-order correction estimated from the wave spectrum is enough to explain the statistics of extremes, and correct the wave spectrum for the presence of lowest order bound wave components (Tayfun, 1980; Janssen, 2009). This correction can also be used to estimate the skewness of the sea surface, a property related to the sea state bias in satellite altimetry (e.g. Elfouhaily et al, 1999). This second order correction also includes the partial standing wave term that makes it possible to measure waves without getting wet, using seismic stations on land (see Ardhuin and Herbers, 2013, for a review of the theory), or acoustic records at large depths (Farrell and Munk, 2008; Ardhuin et al, 2013). There are thus many good reasons to use spectral wave models for the estimation of the second order spectrum. Because this second order spectrum is a function of the full directional (first order) wave spectrum, the measurable second order properties can also be used to validate the shape of the first order spectrum produced by models. Indeed, the full spectrum is almost never available in enough details, except when using dense arrays or techniques such as stereo-video imagery, as illustrated in figure 1.

Wave buoys or co-located combinations of pressure and velocity measurements only provide five parameters for each frequency. The validation of the second order spectrum estimated from a modelled directional spectrum thus provide more information on the width of the peak in the case of sub-harmonics, and on the presence of partial standing waves in the case of the super-harmonics, such as induced by partial reflection (e.g. Touboul and Rey, 2012). However, this second order theory is only valid for a flat bottom and breaks down in shallow water, where it fails to represent the net transfer of energy to free components with shorter periods (super-harmonics) or very long periods (sub-harmonics also known as infragravity waves). A proper representation of these effects requires the use

of a bi-spectrum that carries the relative phase information of the different wave components (e.g. Herbers and Burton, 1997). Several parameterizations have been proposed with some success (Becq-Girard et al, 1999; Toledo et al, 2012), avoiding the higher computational cost incurred when computing the bi-spectrum evolution. These triad nonlinear effects may also be ignored, and accurate significant wave heights can still be obtained (e.g. Thornton and Guza, 1983; Filipot and Ardhuin, 2012), but the the shape of the wave spectrum will not contain the harmonics that have been liberated during propagation over varying topography or currents. We will now focus on the ocean outside of the surf zone.

2.2 Theoretical bases of the wave action equation

Over the last twenty years, models based on the spectral wave action equation (WAE) such as the WAM (WAMDI Group, 1988), TOMAWAC (Benoit et al, 1996), SWAN (Booij et al, 1999), and WW3 (Tolman, 2002b) have gained widespread usage thanks to the versatility of the WAE for including various sources and sinks of energy.

The WAE gives the evolution in space and time of the wave spectrum, represented by the action spectral densities. Assuming linear and irrotational wave theory, it is

$$A(k, \theta) = \frac{E(k, \theta)}{\sigma} = \frac{E(f, \theta)}{2\pi C_g(f, D)\sigma} \quad (1)$$

where σ is the relative radian frequency. The most general form, given by Andrews and McIntyre (1978), is valid for nonlinear and rotational waves, with an intermediate approximation in Willebrand (1975). $C_g(f, D)$ is the group velocity, which for linear waves is only a function of the intrinsic frequency f and water depth D . The wave action is advected at a velocity given by the intrinsic group speed vector $\mathbf{C}_g(f, D)$, which has a norm equal to $C_g(f, D)$ and a direction θ , plus an advective current velocity vector $\mathbf{U}_A(f, \theta)$ which is the generalized Lagrangian mean velocity Andrews and McIntyre (1978). So far, the public versions of numerical models such as SWAN or WW3 do not bother with this kind of detail, and use instead the same surface current velocity vector \mathbf{U} for all spectral components instead of a more general $\mathbf{U}_A(f, \theta)$. For slowly varying depths and currents, the WAE takes the following form,

$$\frac{\partial A(k, \theta)}{\partial t} + \nabla_x [(\mathbf{C}_g(k, \theta) + \mathbf{U}) A(k, \theta)] + \frac{\partial}{\partial k} \dot{k} A(k, \theta) + \frac{\partial}{\partial \theta} \dot{\theta} A(k, \theta) = \frac{S_{\text{tot}}(k, \theta)}{\sigma}, \quad (2)$$

where S_{tot} is the ‘total’ energy source term, involving all processes that contribute to the change of wave energy, except for the adiabatic exchange of energy with varying currents (Phillips, 1977). The WAE is written here on a flat surface and is easily generalized to the curved ocean surface.

The evolution of the action spectrum is further modified by source terms that represent a wide range of processes, including generation by the wind, non-linear evolution of the waves, dissipation by breaking, dissipation by friction at the air-sea interface, bottom friction. Each of these source terms is computed from theoretical bases and empirical adjustments.

Finally, wave propagation can be improved compared to the usual linear waves and geometrical optics approximations. Holthuijsen et al (2003) and Liao et al

(2011) have reproduced some of the diffraction effects that occur in cases where interference from distinct diffraction centres can be neglected, but the full effect of diffraction cannot be reproduced in phase-averaged models. Another regime that is appropriately handled with the WAE is the scattering of waves by random current or depth perturbations (Rayevskiy, 1983; Ardhuin and Magne, 2007). A generalized WAE that takes into account higher order effects of current and depth gradients has been proposed by (Toledo et al, 2012), but it has not yet been implemented into numerical wave prediction models. It should be noted that on natural topographies, even in the presence of very large gradients in the wave field, the effect of diffraction is generally limited (Magne et al, 2007).

2.3 Numerical integration of the wave action equation

Without the source terms, the conservative WAE could be solved exactly by a Lagrangian approach, using ray-tracing methods, with a most practical integration using backward ray tracing (O'Reilly and Guza, 1991). Introducing source terms in ray tracing makes the solution method difficult, in particular if the rays move with time due to changing water levels or currents (Ardhuin et al, 2001). This is simplified by integrating rays over a single time step, as done in the TOMAWAC model Benoit et al (1996), but at the price of some diffusion due to interpolation which may still be much less than the diffusion with a first order finite difference scheme that may be used in other types of models like SWAN or WW3 (Ardhuin and Herbers, 2005). Instead, the unsteady 4-dimensional problem can be formulated in a Eulerian way, as in eq. (2). The left-hand side of that equation can be integrated with common numerical schemes such as finite element methods, finite volume methods, finite difference methods, or residual distribution schemes on either structured or unstructured grids using various time stepping strategies as done in WAM, WW3, SWAN and other models (Roland, 2008). Recent numerical developments have largely focused on the improvement of methods on unstructured grids made of triangular meshes (e.g. Roland, 2008; Zijlema, 2010), the use of quadrangles with variable sizes (Popinet et al, 2010; Li, 2010), or grid nesting (Tolman, 2008). The variability of the grid resolution across the domain exacerbates the problems outlined above.

The solution strategies in these models use either the fractional step method of Yanenko (1971) or solve the problem directly, using implicit time stepping techniques proposed by Patankar (1980). The latter methods form the basis of the SWAN model (Booij et al, 1999), and are very efficient in steady conditions because they do not have a strict CFL-like stability criterion, thus allowing very large time steps. When using large time steps, the solutions are not necessarily accurate.

2.3.1 Wave propagation

The implicit method in SWAN leads to unphysical solutions when waves are strongly refracted over steep slopes (Gonzalez-Lopez et al, 2011), and certain limiters in spectral space must be applied as outlined in Dietrich et al (2013). In that paper, it is mentioned that the turning of the certain wave component within one time step must remain in the quadrant of the current 'sweep'. In practice it should

1 be less than one spectral increment, and similar constraints apply to frequency
2 space when waves go over strong current gradients. The realistic applications with
3 the unstructured version of SWAN (Zijlema, 2010) were obtained by setting the re-
4 fraction term to zero in shallow water (Dietrich et al, 2011), which is the strongest
5 possible limiter.

6 The effect of the Dietrich et al (2013) limiter is evaluated by running the SWAN
7 model on a structured grid using the first order (BSBT Booi et al, 1999) and
8 higher order schemes (SORDUP Rogers et al, 2002), with and without the lim-
9 iter. Here we only show results for the laboratory case of a shoal over a sloping
10 bottom Vincent and Briggs (1989). The water depths are displayed on figure 2.
11 Similar behaviour was found for realistic cases. Figure 3 shows results of these
12 runs. The incoming waves have a period of 1.305 s and a wave height of 5.5 cm.
13 The spatial resolution is 0.2 m for the structured mesh and we used one frequency
14 bin and 240 directional increments in order to represent a monochromatic wave
15 train. This directional resolution is intermediate between the 24 or 36 directions
16 used in most practical application and the 3600 directions used to verify model
17 refraction properties (Ris et al, 2002). With a time step $dt = 0.11$ s that gives
18 a CFL number of 1 for spatial advection, this large number of directions gives a
19 similar CFL for the direction space, here up to 0.49.

20 For this case, depending on the order of the scheme, the influence of these lim-
21 iters may be up to 50% variation of H_s , the significant wave height. In particular
22 the wave height with limiter is lower in the focusing region. Similar differences oc-
23 cur in realistic cases. Looking at the the case of the Haringvliet Estuary (Ris et al,
24 1999; Zijlema, 2010), the limiter results in wave height differences up to 20% with,
25 again, a reduction in the maximum wave heights. As a result, although the lim-
26 iter may guarantee a reasonable model result, removing very large wave spurious
27 heights in the presence of steep slopes, it has a clear impact on the solution.

28 Another particular issue with the implicit methods, comes from the Godunov
29 order barrier theorem (Godunov, 1954). Namely, schemes more accurate than
30 first order must either be non-linear, and very difficult to integrate numerically,
31 or non-monotone. Non-monotone means that in the vicinity of strong gradients,
32 these schemes produce spurious oscillations possibly leading to negative wave en-
33 ergies. This unphysical result can be either eliminated by setting negative values
34 to zero but the scheme loses its conservative properties. In SWAN's, when the
35 SORDUP scheme is used, a 'renormalization' of these negative energies was intro-
36 duced, smoothing them out in the directional space, while keeping the gradients
37 in the physical space. This introduces strong numerical dispersion. This issue is
38 especially visible when looking at parameters such as directional spread, which is
39 already affected by numerical diffusion. In these cases the higher order schemes
40 do not converge to the analytical solution when spectral and spatial resolution is
41 increased (Ardhuin and Herbers, 2005; Roland, 2008).

42 In contrast, fractional step (splitting) methods separate the WAE integration
43 into an ordinary differential equation for the source term integration, and a hy-
44 perbolic partial differential equation for the propagation part. Once separated,
45 specific numerical schemes and solution procedures can be applied most efficiently
46 and accurately for each. This splitting technique gives excellent results in deep
47 ocean and is used in combination with explicit time integration methods for the
48 propagation part in codes such as WW3 or WAM, which are used by most weather
49 forecasting centres. However, in shallow areas, where strong variations of depth
50
51
52
53
54
55
56
57
58
59
60
61
62
63
64
65

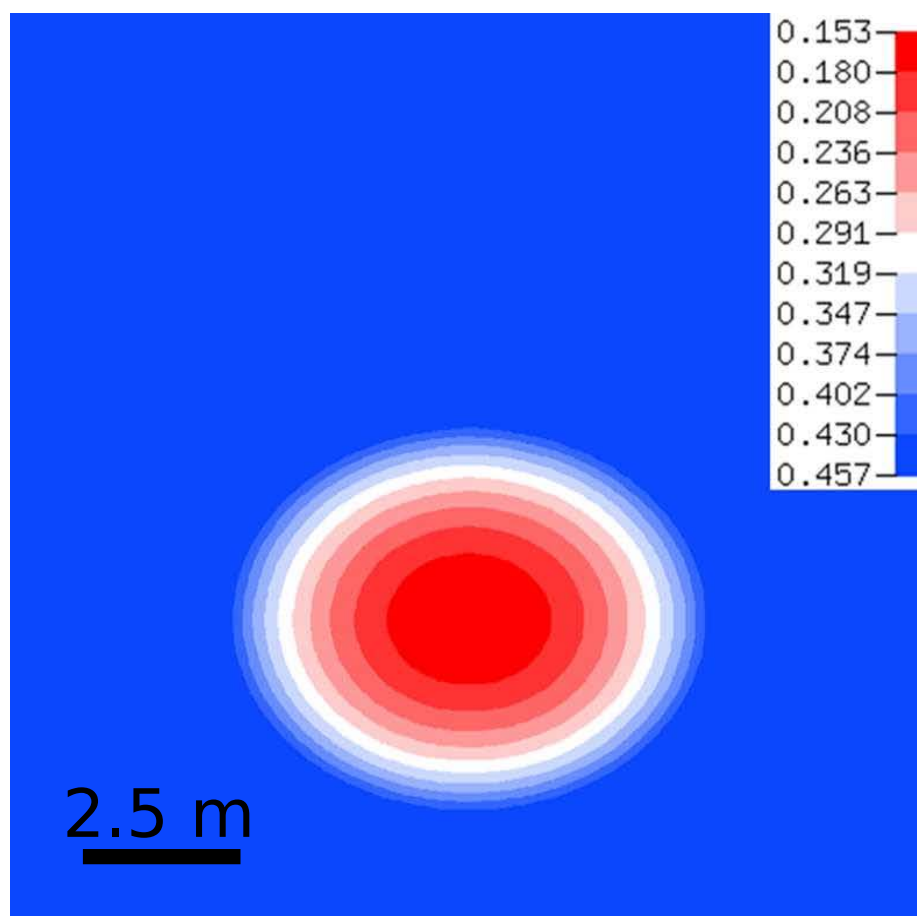


Fig. 2 Depths for the elliptic shoal case, at the laboratory scale of Vincent and Briggs (1989).

and currents have a strong effect on wave propagation, the numerical efficiency of explicit methods is limited by the strict CFL criterion, which may require a very small stable time step for a stable solution. This drawback can be partly circumvented by splitting not only propagation and source terms, but also spectral and geographical advection, and introducing sub-cycling as done in WW3. Hence the time step is only reduced for integrating one term in the WAE equation. In practice, the refraction is also limited in WW3, by the user-defined refraction time step, which was introduced for efficiency and better load-balancing on parallel computing systems. That limiter used to be applied on the depth-induced refraction only, it is now applied, since version 4.05 on the full refraction term, because currents in very shallow water can also lead to very large CFL numbers.

The splitting technique relaxes the time step constraint on the whole system, especially in the presence of steep bottom slopes: the relatively cheap refraction computation can be integrated with a very small step, while the spatial propagation is integrated with its own time step. Due to the sub-cycling, however, splitting

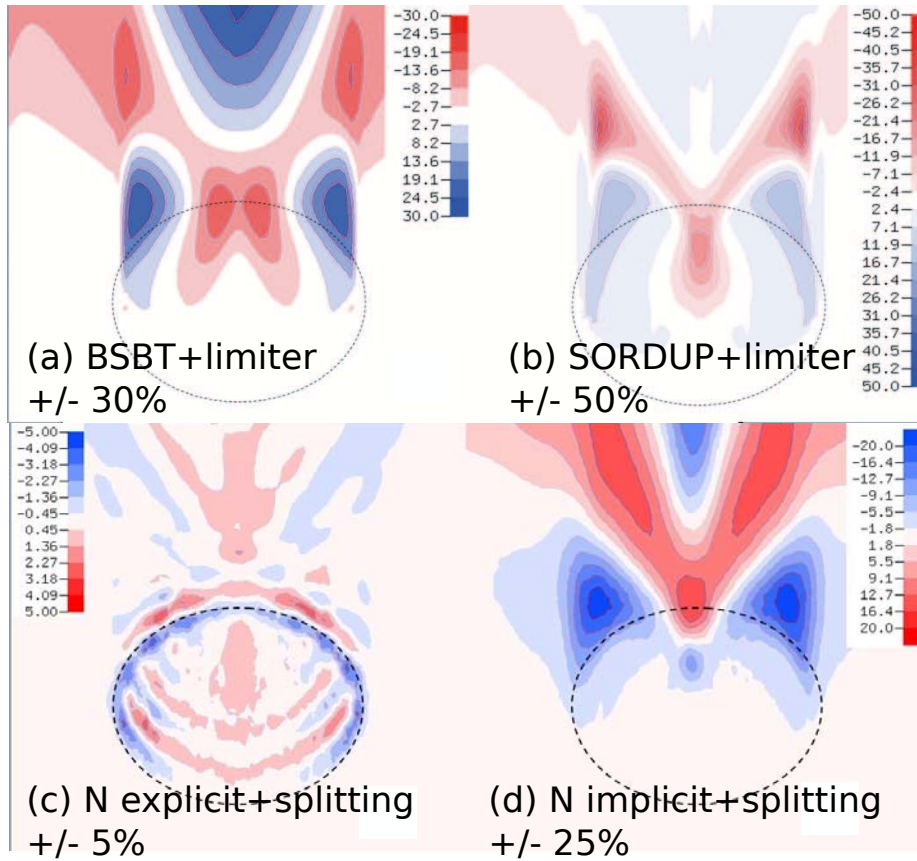


Fig. 3 Impact of numerical schemes on wave heights over the elliptic shoal, illustrated by differences in wave height (in percent). Effect of refraction limiter in the SWAN model with (a) first order BSBT scheme and (b) second order scheme, the colors show the difference between simulations with and without limiter. Effect of splitting errors in WWM-II with (c) an explicit N-scheme and (d) the implicit N-scheme, the colors show the difference between large and small time steps, with 10 sub-cycles for the large time step.

errors are introduced into the solution. Namely, the solution of the split integration is not exactly equal to the solution of a single integration of the whole equation, and the difference grows with the number of sub-cycles (see e.g. Roland, 2008). When the surf zone needs to be resolved, or in some tidal channels, the model stability may require a very small time step. Here implicit methods can be applied for geographical space advection to gain some efficiency, which is an option for unstructured grids in version 4 of WW3, but the splitting error remains.

In order to evaluate the error of splitting we have run the Wind Wave Model-II (hereinafter WWM-II Roland, 2008) for the same case, with the same physical and spectra resolutions. To quantify the splitting error, we have increased the global time step by a factor 10, to $dt_G = 1.1$ s, with a time step of the sub-cycles kept at 0.11 s. The integration in directional space uses the ULTIMATE QUICKEST scheme (Leonard, 1991) and spatial advection is performed by the N-Scheme as

1 implemented in WWM-II and WW3 (Csík et al, 2002; Roland, 2008). With the
2 explicit version of the scheme, the splitting errors does not exceed 5%,
3 whereas the implicit scheme produces errors greater than 20% with a pattern that
4 resembles the limiter effect in SWAN. Hence, limiters and splitting errors may
5 results in large errors. The great benefit of splitting methods is that they converge
6 to the true solution when the time step is reduced, which, in practice may be very
7 expensive in computation time. Explicit schemes produce smaller errors, which
8 is due to the fact that gradients are well captured by the sub-cycling, whereas
9 implicit schemes are more diffusive. The splitting error evaluated here is only due
10 to the separate integration of spatial and spectral advection, and does not exist
11 with methods based on ray tracing. However, when source terms on the right hand
12 side of the WAE are strong, which is the case of wave breaking in shallow water,
13 the splitting error may be even larger and all available methods struggle to solve
14 the WAE efficiently and accurately.
15

16 17 18 19 20 21 *2.3.2 Source terms*

22
23 For the integration of these source terms, all spectral wave models apply an
24 additional limiter, which is either linearized following the Patankar rules (see
25 also Booij et al, 1999) or integrated as an ODE problem within a separate frac-
26 tional step. This limiter was introduced in the integration of the source terms
27 (WAMDI Group, 1988; Hersbach and Janssen, 1999; Hargreaves and Annan, 2000;
28 Tolman, 2002b). Within the splitting method, this limiter is only applied to the
29 source term part when the ODE problem is solved. On the contrary, in direct
30 methods (i.e. joint integration of both left and right-hand sides), the application
31 of the limiter on the full integration, as done in the SWAN model, will limit the
32 sum of all terms including propagation, which may have strong influence on the
33 transient solutions in unsteady environments.

34
35 Selective computations of the various terms and limiters would be a pragmatic
36 engineering solution to reduce the influence of limiters in certain regions and im-
37 pose them in others where the solution is not of major concern. This may well make
38 the schemes inconsistent, and possibly not convergent (Lax and Richtmyer, 1956).
39 A similar problem was already corrected in SWAN (e.g. Zijlema and van der Westhuysen,
40 2005).

41
42 For all these reasons, the solution of the WAE in inhomogeneous environments
43 is a complex problem with many open challenges from the physical and numerical
44 points of view. Dedicated numerical schemes must be investigated to arrive at
45 efficient, stable and accurate integration of wave evolution. The WAE equation can
46 be integrated with higher order implicit methods that are stable and monotone, but
47 which must be nonlinear (Godunov, 1954). Such methods, that can avoid splitting
48 errors and effects of non-monotonicity are under development and results will be
49 reported elsewhere. The specific numerics of wave coupling to ocean circulation
50 models (e.g. Dietrich et al, 2011; Roland et al, 2012) is another area that will
51 require special attention.
52
53
54
55
56
57
58
59
60
61
62
63
64
65

3 Application: from Global to coastal wave modelling

3.1 Boundary conditions from global models

In general the accuracy of wave model results in terms of significant wave height is governed, in decreasing order of importance by

- the accuracy of forcing fields: first the wind (and/or the offshore boundary in cases of nested grids), then the currents, and finally the water levels. This order is reversed where water depths limits the wave height because of breaking; there the water level is the primary control on the sea state.
- the accuracy of source term parameterizations
- the effect numerical schemes.

This order is generally verified for large scales, and the developers of numerical wave models have found it convenient to blame the poor quality of atmospheric models for poor wave model performance, especially in coastal areas (e.g. Cavaleri and Bertotti, 1997). Yet, the performance of operational atmospheric models is improving at a dramatic pace, with errors on wind speed reduced by more than 20% between 1992 and 2006 (Janssen, 2008). With these improvements, it has become increasingly clear that wave model parameterizations could be upgraded. Figure 4 shows the reduction in wave model errors on the significant wave height, when changing the wave generation and dissipation terms from the WAMDI Group (1988), to the ones by Tolman and Chalikov (1996), Bidlot et al (2005) and, possibly the most accurate formulation to date, the one by Ardhuin et al (2010) with a recent update by Rasclé and Ardhuin (2013). That parameterization was a compromise mostly suited to the global scale, and still suffers a weak growth bias at short fetch, which could be corrected by improving on the wind stress parameterization used in the wave generation term. As a result, modellers may prefer the parameterizations of van der Westhuysen et al (2007) or Filipot and Ardhuin (2012) in enclosed areas. This was particularly well demonstrated by Alves et al (2013), in the north-American Great Lakes. Further progress is certainly on the way, with ongoing research projects that are addressing the question of parameterizations (e.g. Tolman et al, 2013).

These improvements have further revealed flaws in the model forcing. In particular the bands of low and high bias along the equatorial Pacific are clearly associated with ocean currents (Rasclé et al, 2008), while icebergs in the southern ocean have been found to be a major source of error if not taken into account (Ardhuin et al, 2011). In the global results shown here, icebergs are represented, but the surface currents are still neglected due to large errors in global ocean circulation models.

The little impact of advanced numerical schemes on the model scores for the significant wave height H_s may be rather discouraging to model developers, but it comes from the smoothing effect of low order schemes. Indeed ECMWF and Meteo-France still use first order upwind scheme similar to the original WAM code (WAMDI Group, 1988), which gives lower r.m.s. errors for H_s in most of the world ocean. However, the third order scheme used here can give much better results when the wave field is partitioned into swells and wind seas and errors on swell heights are considered (Wingear, 2001). Such a scheme, however, requires a careful treatment of the spectral discretization in order to mitigate the 'Garden

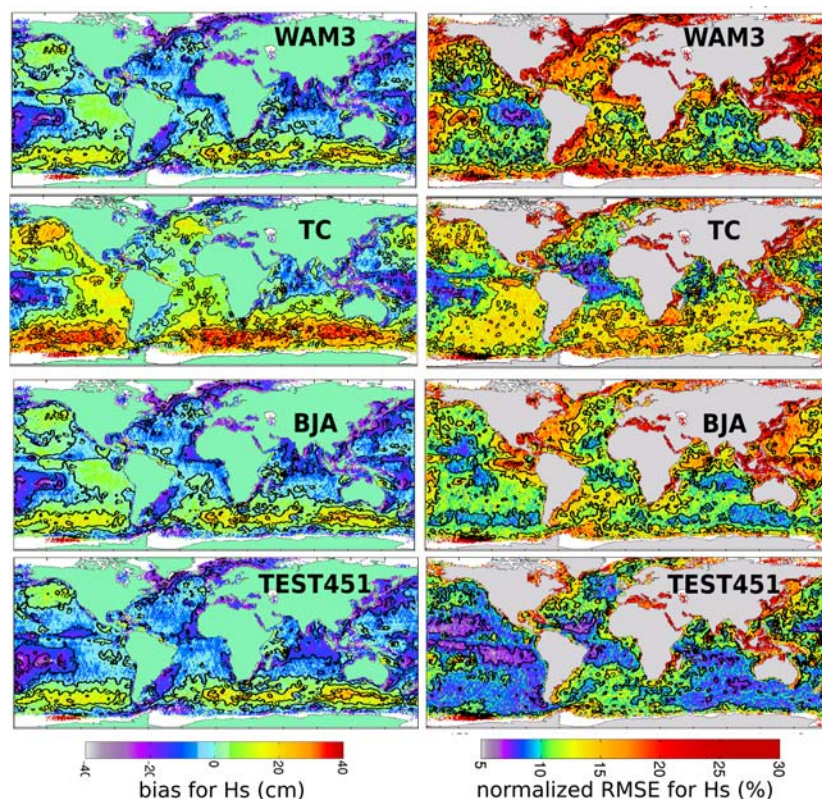


Fig. 4 Bias and normalized RMS error against altimeter data for the year 2007, using the same forcings but 4 different parameterizations of the wind input and dissipation: WAM Cycle 3 (WAMDI 1988), TC (Tolman and Chalikov 1996), BJA (Bidlot et al. 2005) and TEST451 (Rasclé and Ardhuin 2013). Solid lines in the right column correspond to contours at the 7.5, 10, 12.5, 15 and 20% levels.

Sprinkler Effect' that leads to a spatial discretization of the waves propagated from a compact source, because of the spectral discretization (Booij and Holthuijsen, 1987; Tolman, 2002a).

3.2 Coastal seas

When moving towards the coastal ocean, many effects can come into play. For open coasts, the quality of lateral boundary conditions from a global or regional wave model is obviously important because the waves mostly come from the open ocean. In the case of the French Atlantic coast, the TEST451 parameterization (Ardhuin et al, 2010; Rasclé and Ardhuin, 2013) generally produces a 10 to 20% excess of wave energy for wave periods between 12 and 16 s, especially on west coasts. For longer wave periods, up to 25 s, the global wind fields are very important. In particular the ECMWF operational analysis systematically underestimate the highest winds that lead to these very long swells, whereas the CFS-Reanalysis (Saha et al, 2010) and the NCEP operational analysis provide more consistent

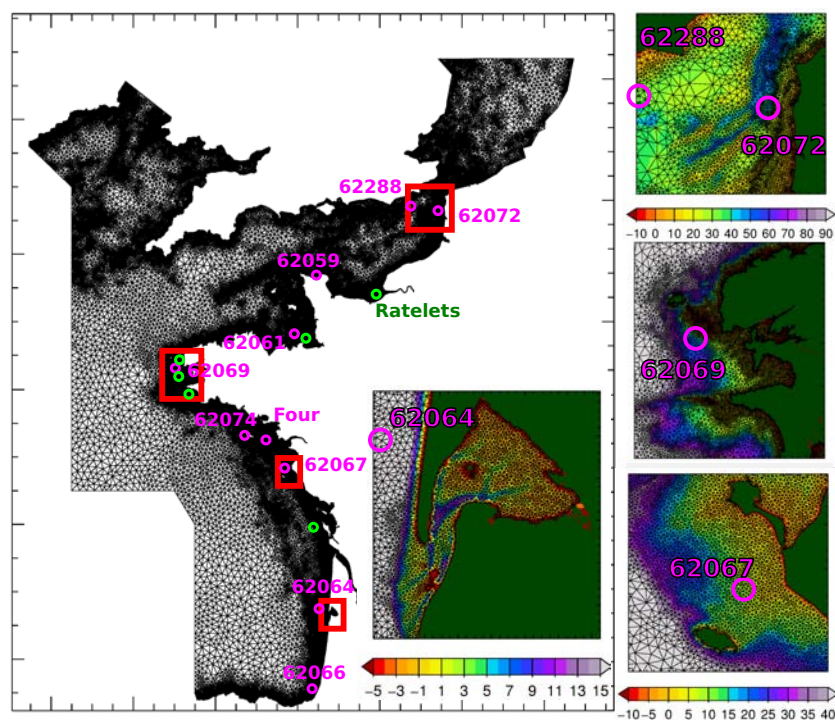


Fig. 5 Map showing the North Sea - Channel - Biscay mesh used for our hindcasts and forecasts. Magenta and green circles show location of permanent and temporary buoys used for calibration or validation in addition to satellite altimeter data. Inset are zooms of four grid areas, showing typical alongshore resolutions, with color bars displaying the elevation relative to mean sea level, in meters. The full mesh contains 110,000 wet nodes.

values in the high wind range. As a result, our hindcasts with ECMWF analyses lead to an underestimation of these long wave components because they are not properly generated in the deep ocean. For example, the Quirin storm with the highest-ever measured sea state on February 15, 2011 (Hanafin et al, 2012), gave swell heights of 3.8 m at buoy 62074 when considering periods larger than 20 s, when these did not exceed 2 m in the model forced by ECMWF analyses.

Coastal areas are often influenced by strong currents, driven by either tides or water density gradients. Recent works have shown that wave model results can be strongly improved by taking into account currents, and their effects on wave refraction, enhanced wave breaking and change in relative wind speeds (van der Westhuysen et al, 2012; Ardhuin et al, 2012). Another important effect, when the water depth is less than half the dominant wavelength, is bottom friction. It has been known for decades that bottom friction may lead to strong wave energy dissipation (e.g. Shemdin et al, 1980), reducing the wave height by as much as a factor 3 in some conditions (Ardhuin et al, 2003b). Still, a physically-based parameterization of this effect had not been introduced into mainstream spectral wave models until now. Here we particularly discuss the implementation in WW3 of the movable-bed bottom friction proposed by Tolman (1994) and adjusted using data from the Shoaling Waves Experiment (SHOWEX Ardhuin et al, 2003b).

3.3 The IOWAGA hindcast and Previmer forecasting system

Model implementation Based on the same WW3 code already used for the global ocean, we have used a 110,000 node unstructured mesh with an along-shore resolution of 300 to 500 m, shown in figure 6. This WW3 model configuration uses 32 frequencies from 0.037 to 0.72 Hz and 24 directions. It is forced at the boundary by the output of a multi-grid WW3 system that combines 0.5 and 0.15° resolution grids for our region of interest (Rascle and Ardhuin, 2013). The WAE is integrated in parts over 180 s steps. The spatial propagation part uses the N-scheme for the (Csík et al, 2002; Roland, 2008), with a maximum time step of 60 s for the sub-cycles, dynamically adapted for each spectral component but always more than 15 s. The source terms are integrated with a variable time step that can be as low as 5 s. Most of the cost of the calculation lies with the advection.

This model is forced by operational ECMWF wind analysis at a resolution of 0.25 degree or better, with a time step of 6 hours (3 hours since January 2013, thanks to the combination of forecasts and analyses). Currents and water levels on a series of grids with a resolution of 200 m is provided by the Previmer system based on the MARS2D model. A map of median grain size has been established from the French Hydrographic Service (SHOM) database (Garlan, 1995, 2009).

Model results can be viewed on the wave modelling page of <http://www.previmer.org>, with numerical results available at <http://tinyurl.com/iowagaftp>, including full spectra for over 4000 grid points, and the full frequency spectrum over the entire grid. At this spatial resolution, the refraction over shoals and tidal currents, and the sheltering by islands and headlands are accurately represented (Ardhuin et al, 2013). The same model settings have been used with CFSR winds for a 20-year hindcast also available (Bouidière et al, 2013).

Calibration and validation of bottom friction A preliminary analysis of all the available buoy data showed an anomalous behaviour for the Yeu buoy (WMO number 62067), with measured wave energies much lower than predicted using the bottom friction parameterization loosely derived from the JONSWAP experiment (Hasselmann et al, 1973; Bouws and Komen, 1983), or the SHOWEX movable bed friction using medium sand grain sizes (Ardhuin et al, 2003a). These measurements are also confirmed by the few good data, between Yeu Island and the mainland, from the Jason-1 altimeter track. In fact, an inspection of the sediment cover reveals that the buoy lies down-wave of a 20 km-wide region of shallow rock platforms (figure 6).

We have thus taken into account the bottom types, particularly sand, gravel and rocks. We started from the SHOWEX parameterization for movable beds, with which WW3 was verified to reproduce the ray-tracing results obtained by Ardhuin et al (2003a) for the North Carolina shelf. That parameterization was modified to give a constant Nikuradse roughness for rock bottoms. This roughness value was tuned here to 12 cm in order to reproduce the observed wave heights. This value was applied to all rocky areas. This modified bottom friction has limited impact at other locations (figure 7, and table 1). Such a large roughness value was also found to improve model results for waves crossing the rocky platform to the west of Sein island (not shown). Overall the SHOWEX bottom friction yields lower wave heights in very shallow water and results that are quite close to the JONSWAP results in intermediate water depths.

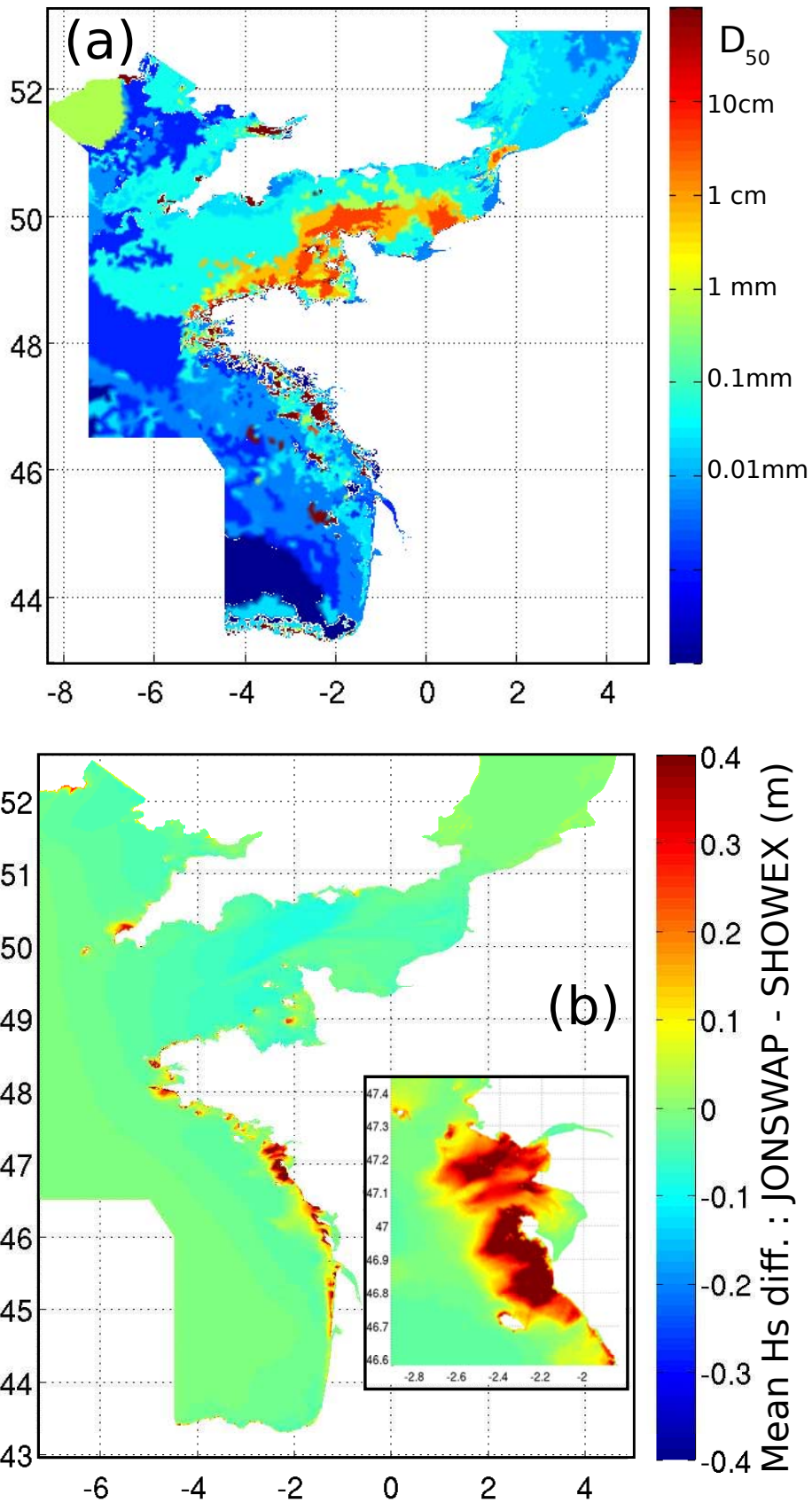


Fig. 6 (a) Map of sediment median diameter and (b) mean difference in significant wave height (in meters) over the month of February 2010 between a model run using the 'JONSWAP' bottom friction parameterization and another using the 'SHOWEX' parameterization with a constant Nikuradse roughness length of 12 cm for rocks. Inset is a zoom on the region around Yeu and Noirmoutier islands where the impact of this friction is very clear, as also shown in figure 7.a.

Table 1 Statistics of model errors for the significant wave height H_s against buoy data for the NORASUG model grid for the months of February and March 2011, using either the JONSWAP (BT1) or SHOWEX (BT4) parameterizations for bottom friction. S.I. stands for scatter index, while N.B. is the bias normalized by the RMS observed value. Both are given in percent.

buoy	longitude	latitude	BT1, S.I.	BT1, N.B.	BT4, S.I.	BT4 N.B.
Four	-2.78	47.24	14.4	5.91	13.9	5.03
62064	-1.45	44.65	11.4	3.2	11.3	4.0
62066	-1.61	43.53	18.6	-6.5	18.2	-5.0
62067	-2.29	46.83	22.2	25.3	8.9	6.8
62069	-4.9	48.28	11.3	1.3	11.4	1.0
62059	-1.62	49.70	19.0	23.7	17.3	23.6
62072	1.37	50.66	24.4	4.1	25.0	0.5
62074	-3.3	47.3	10.8	-1.7	10.8	-2.1
62288	0.75	50.75	18.2	1.9	18.1	1.2

Table 1 shows that differences between the JONSWAP and SHOWEX parameterizations are significant only at buoys 62067 and 62059. Other buoys are generally in deeper water, or exposed to relatively shorter wave periods for which bottom friction is not so important. This table also reveals that errors with the SHOWEX parameterization are largest at buoys 62072, located only 2 km from the breakwaters that protect the harbour of Cherbourg. At that location the maximum tidal range is 7 m. Currents as large as 1.5 m could be causing problems with the performance of the Datawell buoy, but the spectra look reasonable even during spring tides. Instead, it is likely that current gradients may not be well resolved in the tidal model or that their effect is not well represented in the wave model, unlike what was found for the region around buoy 62069 (Ardhuin et al, 2012). All these buoy results are consistent with the differences between model and altimeter data (figure 8), which are very useful for identifying regions with particular problems. For example, the North Sea suffers from a low bias which comes from the general short fetch bias in the chosen parameterization, and, possibly, an exaggerated bottom friction. This area will require further attention.

Effect of coastal reflection In the Eastern Channel at buoy 62288 (Hastings) and 62072 (Vergoyer), waves are too short to be significantly modified by bottom friction, and the wave heights are generally underestimated by a few percent. This error may be largely due to an underestimation of waves at short fetch with the wind-wave growth parameterization of Ardhuin et al (2010). At that site, however, we have found a beneficial impact of adding reflection off the shoreline, taking a uniform shoreface slope of 30% to account for the steep beaches and cliffs, and using the parameterization by Ardhuin and Roland (2012). Compared to our baseline model run, the bias on wave heights was changed from 0.5% to 2.5%. The directional properties were also improved by this added reflection, especially for the higher frequency range (0.15 to 0.4 Hz) with a significant reduction of the r.m.s. error on the mean direction, from 47 to 42 degrees, and a strong reduction the bias and scatter index for the directional spread. These results are consistent with the model improvements reported for the U.S. West coast by Ardhuin and Roland (2012). We are waiting to assemble a database of shoreline slopes in order to implement this parameterization in our routine hindcasts and forecasts. This was

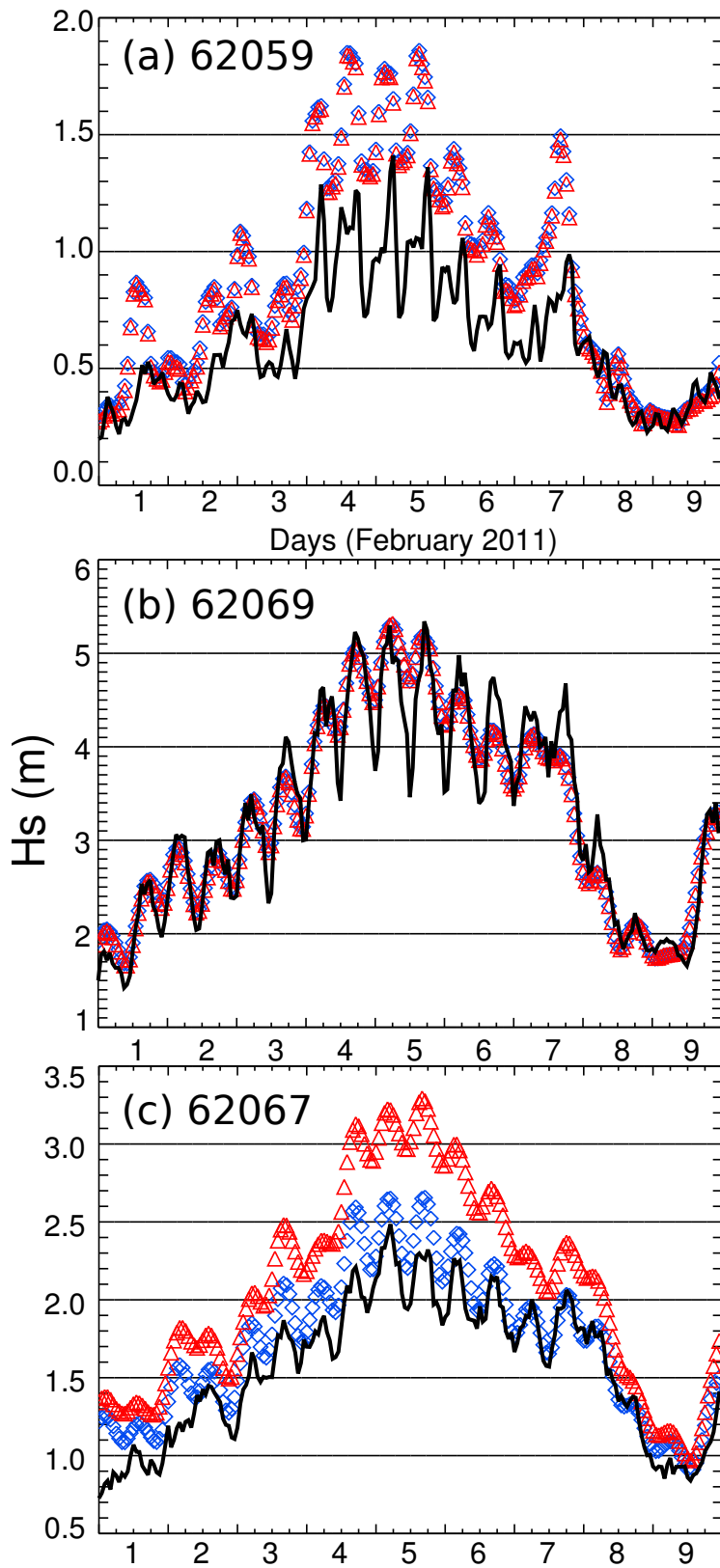


Fig. 7 Time series of observed and modelled significant wave height at several buoys using the JONSWAP (blue diamonds) or SHOWEX (red triangles) parameterizations for bottom friction, compared to hourly buoy measurements (solid line).

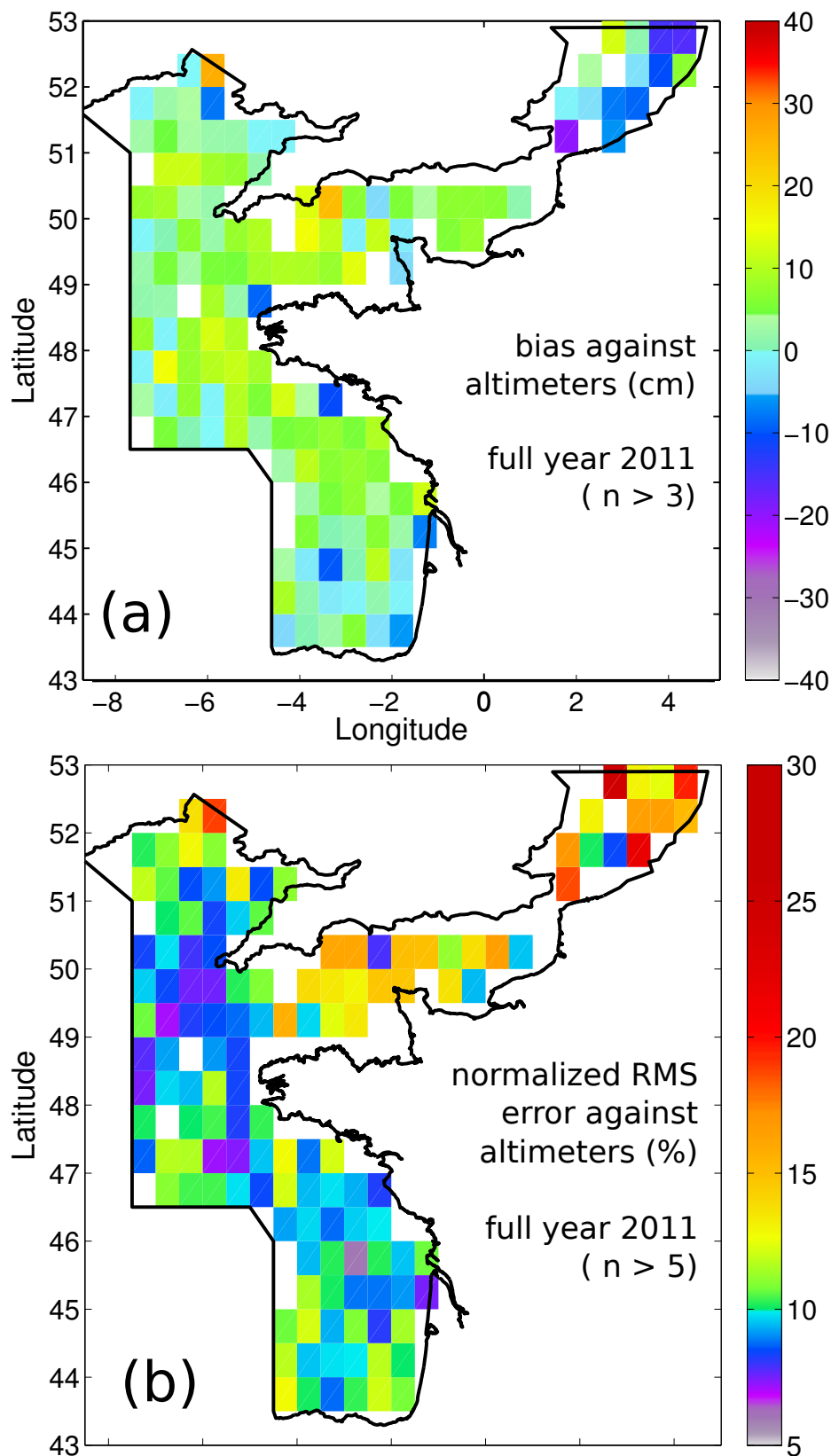


Fig. 8 Validation of the bay of Biscay model grid for year 2011 using all available altimeter data. (a) bias in centimeters, and (b) normalized root mean square error (NRMSE). The satellite data was taken from the calibrated Ifremer database (Queffeuou and Croizé-Fillon, 2010). The along-track time series at 1 Hz sampling was averaged over 0.5 degree along the track. These 'super-observations' (SO) were then binned with latitude and longitude, with an average number of 35 SOs for one year in each 0.5 by 0.5 degree bin. Results are only shown for bins with at least 4 SOs for the bias and 6 SOs for the NRMSE.

1 done for most of the U.S. West coast using 1-m resolution lidar data. Data with
2 such an extensive coverage are not yet available in Europe.
3
4
5
6

7 **4 Summary and perspectives**

8
9 Numerical wave models have evolved dramatically over the last two decades. Their
10 accuracy has increased thanks to improvements in forcing fields and parameteri-
11 zations, and they are now more capable of handling complex coastal topographies
12 with numerical schemes that are efficient on small computer cluster or massively
13 parallel machines.

14 A landmark in this progress will certainly be the version 4.18 of the WAVE-
15 WATCH III code now available from the National Centers for Environmental Pre-
16 diction (NOAA/NCEP). This wave modelling framework has been augmented with
17 many features, including improved parameterizations of wave generation and dis-
18 sipation, bottom friction, coastal reflection. The new code handles curvilinear,
19 sperical multiple cell grids, and triangle-based meshes (e.g. Ardhuin et al, 2012).
20 The latter type of grid has been thoroughly tested with 20-year hindcasts and rou-
21 tine forecasts. Here we have used the explicit N-scheme on triangle meshes, because
22 it is faster than higher order explicit schemes, and its larger diffusion gives weaker
23 discretization effects known as the ‘garden sprinkler effect’. This explicit scheme
24 also gives smaller errors than its implicit version. The four different schemes for
25 unstructured grids are available to users. There are trade-offs between model ac-
26 curacy and its computational cost in the choice of numerical scheme or the choice
27 between fractional step (splitting) methods and non-splitting methods. As for the
28 cost, in our North Sea - Channel - Biscay mesh the spatial advection with the N
29 scheme only accounts for 22% of the total computation cost. By allowing to put
30 more nodes where there are gradients in the wave field, the irregular grids allow a
31 much faster simulation than a regular grids with high resolution everywhere, and
32 that efficiency mostly come from the reduction in the number of nodes and thus
33 in the time needed to compute source terms.
34

35 In WAVEWATCH III, the different grid types can be two-way nested is a
36 single multi-grid system. The code also allows coupling using generic couplers
37 (Bennis et al, 2011), or off-line forcing with all the necessary two or three-dimensional
38 fields. Many new applications are made possible by the greater accuracy of the
39 shape of the wave spectrum, from remote sensing to seismology, and these new
40 applications are providing error estimates that will in turn allow to refine the
41 source term parameterizations (Rasclé and Ardhuin, 2013; Ardhuin et al, 2013).

42 Beyond the wave model itself, the basic numerical tools needed to investigate
43 complex wave-current interaction problems are now available. The first benefit
44 of these efforts will certainly be an improved wind and current forcing for the
45 wave models, opening many exciting perspectives. From air-sea fluxes to sedi-
46 ment transport and the interpretation of remote sensing data, many applications
47 can be found. Yet, the numerical schemes that are used up to know on unstruc-
48 tured meshes need further developments in order to be efficient and accurate in
49 the nearshore, at resolutions smaller than 100 m, especially when coupled with
50 circulation models.
51
52
53
54
55
56
57
58
59
60
61
62
63
64
65

Acknowledgements This work was made possible by the help and dedication of many, including J. Lepesqueur who generated the bottom type files and performed the initial simulations with variable roughness. All altimeter data processed by P. Queffeuou was kindly provided by CNES, ESA and NOAA. We thank CETMEF, CEFAS, and SHOM for providing the buoy data, and the organizers of Coastal Dynamics 2013 for soliciting this contribution. A.R. is funded by SHOM, F.A. is funded by ERC grant #240009 'IOWAGA' with additional support from the U.S. National Ocean Partnership Program, under grant N00014-10-1-0383 and Labex Mer via grant ANR-10-LABX-19-01. A. Sepulveda kindly gave feedback on a draft of the manuscript.

References

- Alves JHGM, Chawla A, Tolman HL, Schwab D, Lang G, Mann G (2013) The operational implementation of a great lakes wave forecasting system at noaa/ncep. *Weather and Forecasting* 28:in press
- Andrews DG, McIntyre ME (1978) On wave action and its relatives. *J Fluid Mech* 89:647–664, corrigendum: vol. 95, p. 796
- Ardhuin F, Herbers THC (2005) Numerical and physical diffusion: Can wave prediction models resolve directional spread? *J Atmos Ocean Technol* 22(7):886–895
- Ardhuin F, Herbers THC (2013) Double-frequency noise generation by surface gravity waves in finite depth: gravity, acoustic and seismic modes. *J Fluid Mech* 716:316–348
- Ardhuin F, Magne R (2007) Current effects on scattering of surface gravity waves by bottom topography. *J Fluid Mech* 576:235–264
- Ardhuin F, Roland A (2012) Coastal wave reflection, directional spreading, and seismo-acoustic noise sources. *J Geophys Res* 117:C00J20, DOI 10.1029/2011JC007832
- Ardhuin F, Roland A (2013) spectral wave models, coastal and coupled aspects. In: Bonneton P, Garlan T (eds) *Coastal Dynamics '13*, University of Bordeaux, pp 25–38
- Ardhuin F, Herbers THC, O'Reilly WC (2001) A hybrid Eulerian-Lagrangian model for spectral wave evolution with application to bottom friction on the continental shelf. *J Phys Oceanogr* 31(6):1498–1516
- Ardhuin F, Herbers THC, Jessen PF, O'Reilly WC (2003a) Swell transformation across the continental shelf. part II: validation of a spectral energy balance equation. *J Phys Oceanogr* 33:1940–1953
- Ardhuin F, O'Reilly WC, Herbers THC, Jessen PF (2003b) Swell transformation across the continental shelf. part I: Attenuation and directional broadening. *J Phys Oceanogr* 33:1921–1939
- Ardhuin F, Rogers E, Babanin A, Filipot JF, Magne R, Roland A, van der Westhuysen A, Queffeuou P, Lefevre JM, Aouf L, Collard F (2010) Semi-empirical dissipation source functions for wind-wave models: part I, definition, calibration and validation. *J Phys Oceanogr* 40(9):1917–1941
- Ardhuin F, Stutzmann E, Schimmel M, Mangeney A (2011) Ocean wave sources of seismic noise. *J Geophys Res* 116:C09,004, DOI 10.1029/2011JC006952,
- Ardhuin F, Balanche A, Stutzmann E, Obrebski M (2012) From seismic noise to ocean wave parameters: general methods and validation. *J Geophys Res* 117:C05,002, DOI 10.1029/2011JC007449
- Ardhuin F, Lavanant T, Obrebski M, Marié L, Royer JY, d'Eu JF, Howe BM, Lukas R, Aucan J (2013) A numerical model for ocean ultra low frequency

- 1 noise: wave-generated acoustic-gravity and Rayleigh modes. *J Acoust Soc Amer*
2 In press
- 3 Becq-Girard F, Forget P, Benoit M (1999) Non-linear propagation of unidirectional
4 wave fields over varying topography. *Coastal Eng* 38:91–113
- 5 Benetazzo A (2006) Measurements of short water waves using stereo matched
6 image sequences. *Coastal Eng* 53:1013–1032
- 7 Bennis AC, Ardhuin F, Dumas F (2011) On the coupling of wave and three-
8 dimensional circulation models : Choice of theoretical framework, practical im-
9 plementation and adiabatic tests. *Ocean Modelling* 40:260–272
- 10 Benoit M, Marcos F, Becq F (1996) Development of a third generation shallow-
11 water wave model with unstructured spatial meshing. In: *Proceedings of the 25th*
12 *International Conference on Coastal Engineering*, Orlando, ASCE, pp 465–478
- 13 Bidlot J, Janssen P, Abdalla S (2005) A revised formulation for ocean wave dissipa-
14 tion in CY25R1. Tech. Rep. Memorandum R60.9/JB/0516, Research Depart-
15 ment, ECMWF, Reading, U. K.
- 16 Booij N, Holthuijsen LH (1987) Propagation of ocean waves in discrete spectral
17 wave models. *J Comp Phys* 68:307–326
- 18 Booij N, Ris RC, Holthuijsen LH (1999) A third-generation wave model for coastal
19 regions. 1. model description and validation. *J Geophys Res* 104(C4):7,649–7,666
- 20 Boudière E, Maisondieu C, Ardhuin F, Accensi M, Pineau-Guillou L, Lepesqueur
21 J (2013) A suitable metocean hindcast database for the design of Marine energy
22 converters. *Int J Mar Energy* 28:e40–e52
- 23 Bouws E, Komen GJ (1983) On the balance between growth and dissipation in
24 an extreme depth-limited wind-sea in the southern North Sea. *J Phys Oceanogr*
25 13:1653–1658
- 26 Cavaleri L, Bertotti L (1997) In search of the correct wind and wave fields in a
27 minor basin. *Mon Weather Rev* 125(8):1964–1975
- 28 Csík Á, Ricchiuto M, Deconinck H (2002) A conservative formulation of the mul-
29 tidimensional upwind residual distribution schemes for general nonlinear con-
30 servation laws. *J Comp Phys* 172(2):286–312
- 31 Dietrich JC, Westerink JJ, Kennedy AB, Smith JM, Jensen RE, Zijlema M,
32 Holthuijsen LH, Dawson C, Luettich RA Jr, Powell MD, Cardone VJ, Cox
33 AT, Stone GW, Pourtaheri H, Hope ME, Tanaka S, Westerink LG, Westerink
34 HJ, Cobell Z (2011) Hurricane gustav (2008) waves and storm surge: Hind-
35 cast, synoptic analysis, and validation in southern louisiana. *Mon Weather Rev*
36 139:2488–2522
- 37 Dietrich JC, Zijlema M, Allier PE, Holthuijsen LH, Booij N, Meixner JD, Proft
38 JK, Dawson CN, Bender CJ, Naimaster A, Smith JM, Westerink JJ (2013)
39 Limiters for spectral propagation velocities in SWAN. *Ocean Modelling* 139:85–
40 102, DOI 10.1016/j.ocemod.2012.11.005
- 41 Dommermuth D, Yue D (1987) A high-order spectral method for the study of
42 nonlinear gravity waves. *J Fluid Mech* 184:267–288
- 43 Elfouhaily T, Thompson D, Vandemark D, Chapron B (1999) Weakly nonlinear
44 theory and sea state bias estimations. *J Geophys Res* 104(C4):7641–7647
- 45 Farrell WE, Munk W (2008) What do deep sea pressure fluctuations tell
46 about short surface waves? *Geophys Res Lett* 35(7):L19,605, DOI 10.1029/
47 2008GL035008
- 48 Filipot JF, Ardhuin F (2012) A unified spectral parameterization for wave break-
49 ing: from the deep ocean to the surf zone. *J Geophys Res* 117:C00J08, DOI
50
- 51
52
53
54
55
56
57
58
59
60
61
62
63
64
65

- 10.1029/2011JC007784
- Garlan T (1995) La cartographie des sédiments du littoral français. résultats et objectifs. *J Rech Océanogr* 20:50–54
- Garlan T (2009) De la classification des sédiments à la cartographie de la nature des fonds marins. *Annales Hydrographiques* 20:50–54
- Godunov SK (1954) Different methods for shock waves. PhD thesis, Moscow State University
- Gonzalez-Lopez JO, Westerink J, Mercado A, Capella J, Morell J, Canals M (2011) Effect of a steep and complex-featured shelf on computed wave spectra. In: Proceedings, 12th Int. Workshop of Wave Hindcasting and Forecasting, Hawaii
- Hanafin J, Quilfen Y, Ardhuin F, Vandemark D, Chapron B, Feng H, Sienkiewicz J, Queffelec P, Obrebski M, Chapron B, Reul N, Collard F, Cormand D, de Azevedo EB, Vandemark D, Stutzmann E (2012) Phenomenal sea states and swell radiation: a comprehensive analysis of the 12–16 February 2011 North Atlantic storms. *Bull Amer Meteorol Soc* 93:1825–1832
- Hargreaves JC, Annan JD (2000) Comments on –improvement of the short-fetch behavior in the wave ocean model (WAM)–. *J Atmos Ocean Technol* 18:711–715
- Hasselmann K, Barnett TP, Bouws E, Carlson H, Cartwright DE, Enke K, Ewing JA, Gienapp H, Hasselmann DE, Kruseman P, Meerburg A, Müller P, Olbers DJ, Richter K, Sell W, Walden H (1973) Measurements of wind-wave growth and swell decay during the Joint North Sea Wave Project. *Deut Hydrogr Z* 8(12):1–95, suppl. A
- Herbers THC, Burton MC (1997) Nonlinear shoaling of directionally spread waves on a beach. *J Geophys Res* 102(C9):21,101–21,114
- Hersbach H, Janssen PAEM (1999) Improvement of the short-fetch behavior in the wave ocean model (WAM). *J Atmos Ocean Technol* 16:884–892.
- Holthuijsen LH, Herman A, Booij N (2003) Phase-decoupled refraction-diffraction for spectral wave models. *Coastal Eng* 49:291–305
- Janssen PAEM (2008) Progress in ocean wave forecasting. *J Comp Phys* 227:3572–3594, DOI doi:10.1016/j.jcp.2007.04.029
- Janssen PAEM (2009) On some consequences of the canonical transformation in the Hamiltonian theory of water waves. *J Fluid Mech* 637:1–44
- Komen GJ, Cavaleri L, Donelan M, Hasselmann K, Hasselmann S, Janssen PAEM (1994) Dynamics and modelling of ocean waves. Cambridge University Press, Cambridge
- de Laplace PS (1776) Suite des recherches sur plusieurs points du système du monde (XXV–XXVII). *Mém Présentés Acad R Sci Inst France* pp 542–552
- Lax PD, Richtmyer RD (1956) Survey of the stability of linear finite difference equations. *Comm Pure Appl Math* 9:267–293
- Leonard BP (1991) The ULTIMATE conservative difference scheme applied to unsteady one-dimensional advection. *Computational Methods in Applied Mechanical Engineering* 88:17–74
- Li JG (2010) Global transport on a spherical multiple-cell grid. *Mon Weather Rev* 139:1536–1555, DOI <http://dx.doi.org/10.1175/2010MWR3196.1>
- Liau JM, Roland A, Hsu TW, Ou SH, Li YT (2011) Wave refraction-diffraction effect in the wind wave model WWM. *Coastal Eng* 58:429–443
- Magne R, Belibassakis K, Herbers THC, Ardhuin F, O’Reilly WC, Rey V (2007) Evolution of surface gravity waves over a submarine canyon. *J Geophys Res* 112:C01,002, DOI 10.1029/2005JC003035

- 1 O'Reilly WC, Guza RT (1991) Comparison of spectral refraction and refraction-
2 diffraction wave models. *J of Waterway, Port Coast Ocean Eng* 117(3):199–215
- 3 Patankar S (1980) Numerical heat transfer and fluid flow: Computational methods
4 in mechanics and thermal science. Hemisphere Publishing Corp., Washington,
5 DC
- 6 Phillips OM (1977) The dynamics of the upper ocean. Cambridge University Press,
7 London, 336 p.
- 8 Popinet S, Gorman RM, Rickard GJ, Tolman HL (2010) A quadtree-adaptive
9 spectral wave model. *Ocean Modelling* 34:36–49
- 10 Priestley MB (1965) Evolutionary and non-stationary processes. *J Roy Statist Soc*
11 *Ser B* 27:204–237
- 12 Queffelec P, Croizé-Fillon, D (2010) Global altimeter SWH data set, Version 7,
13 Ifremer, France.
- 14 Rasclé N, Ardhuin F (2013) A global wave parameter database for geophysical
15 applications. part 2: model validation with improved source term parameteriza-
16 tion. *Ocean Modelling* in press, DOI 10.1016/j.ocemod.2012.12.001
- 17 Rasclé N, Ardhuin F, Queffelec P, Croizé-Fillon D (2008) A global wave pa-
18 rameter database for geophysical applications. part 1: wave-current-turbulence
19 interaction parameters for the open ocean based on traditional parameteriza-
20 tions. *Ocean Modelling* 25:154–171
- 21 Rayevskiy MA (1983) On the propagation of gravity waves in randomly inhomog-
22 eneous nonsteady-state currents. *Izv Atmos Ocean Phys* 19(6):475–479
- 23 Ris R, Holthuijsen LH, Smith JM, Booij N, van Dongeren AR (2002) The onr
24 virtual testbed for coastal and oceanic wave models. In: *Proc. 28th Int. Conf.*
25 *Coastal Engng., ASCE, Cardiff, ASCE*, pp 380–391
- 26 Ris RC, Booij N, Holthuijsen LH (1999) A third-generation wave model for coastal
27 regions. 2. verification. *J Geophys Res* 104(C4):7,667–7,681
- 28 Rogers WE, Kaihatu JM, Petit HAH, Booij N, Holthuijsen LH (2002) Diffusion
29 reduction in an arbitrary scale third generation wind wave model. *Ocean Eng*
30 29:1357–1390
- 31 Roland A (2008) Development of WWM II: Spectral wave modelling on unstruc-
32 tured meshes. PhD thesis, Technische Universität Darmstadt, Institute of Hy-
33 draulic and Water Resources Engineering
- 34 Roland A, Zhang YJ, Wang HV, Meng Y, Teng YC, Maderich V, Brovchenko
35 I, Dutour-Sikiric M, Zanke U (2012) A fully couple 3d wave-current interac-
36 tion model on unstructured grids. *J Geophys Res* 117:C00J33, DOI 10.1029/
37 2012JC007952
- 38 Saha S, Moorthi S, Pan HL, Wu X, Wang J, Nadiga S, Tripp P, Kistler R, Woollen
39 J, Behringer D, Liu H, Stokes D, Grumbine R, Gayno G, Wang J, Hou YT,
40 ya Chuang H, Juang HMHaJS, Iredell M, Treadon R, Kleist D, Delst PV, Keyser
41 D, Derber J, Ek M, Meng J, Wei H, Yang R, Lord S, van den Dool H, Kumar
42 A, Wang W, Long C, Chelliah M, Xue Y, Huang B, Schemm JK, Ebisuzaki W,
43 Lin R, Xie P, Chen M, Zhou S, Higgins W, Zou CZ, Liu Q, Chen Y, Han Y,
44 Cucurull L, Reynolds RW, Rutledge G, Goldberg M (2010) The NCEP Climate
45 Forecast System Reanalysis. *Bull Amer Meterol Soc* 91:1015–1057
- 46 Shemdin OH, Hsiao SV, Carlson HE, Hasselmann K, Schulze K (1980) Mechanisms
47 of wave transformation in finite depth water. *J Geophys Res* 85(C9):5012–5018
- 48 SWAMP Group (1984) Ocean wave modelling. Plenum Press, New York
- 49
50
51
52
53
54
55
56
57
58
59
60
61
62
63
64
65

- 1 Tanaka M (2001) Verification of Hasselmann's energy transfer among surface grav-
2 ity waves by direct numerical simulations of primitive equations. *J Fluid Mech*
3 444:199–221
- 4 Tayfun A (1980) Narrow-band nonlinear sea waves. *J Geophys Res* 85(C3):1543–
5 1552
- 6 Fedele F, Tayfun A (2007) Wave height distributions and nonlinear effects. *Ocean*
7 *Engng* 34:1631–1649
- 8 Thornton EB, Guza RT (1983) Transformation of wave height distribution. *J Geo-*
9 *phys Res* 88(C10):5,925–5,938
- 10 Toledo Y, Hsu TW, Roland A (2012) Extended time-dependent mild-slope and
11 wave-action equations for wave-bottom and wave-current interactions. *Proc Roy*
12 *Soc Lond A* 468:184–205, DOI 10.1098/rspa.2011.037
- 13 Tolman HL (1994) Wind waves and moveable-bed bottom friction. *J Phys*
14 *Oceanogr* 24:994–1,009
- 15 Tolman HL (2002a) Alleviating the garden sprinkler effect in wind wave models.
16 *Ocean Modelling* 4:269–289
- 17 Tolman HL (2002b) Distributed memory concepts in the wave model WAVE-
18 WATCH III. *Parallel Computing* 28:35–52
- 19 Tolman HL (2008) A mosaic approach to wind wave modeling. *Ocean Modelling*
20 25:35–47, DOI 10.1016/j.ocemod.2008.06.005
- 21 Tolman HL (2009) User manual and system documentation of WAVEWATCH-
22 IIITM version 3.14. Tech. Rep. 276, NOAA/NWS/NCEP/MMAB
- 23 Tolman HL, Chalikov D (1996) Source terms in a third-generation wind wave
24 model. *J Phys Oceanogr* 26:2497–2518
- 25 Tolman HL, Banner ML, Kaihatu JM (2013) The NOPP operational wave model
26 improvement project. *Ocean Modelling* 70:2–10, DOI 10.1016/j.ocemod.2012.
27 11.011
- 28 Touboul J, Rey V (2012) Bottom pressure distribution due to wave scattering near
29 a submerged obstacle. *J Fluid Mech* 702:444–459
- 30 Vincent CL, Briggs MJ (1989) Refraction-diffraction of irregular waves over a
31 mound. *J of Waterway, Port Coast Ocean Eng* 115:269–284
- 32 WAMDI Group (1988) The WAM model - a third generation ocean wave prediction
33 model. *J Phys Oceanogr* 18:1775–1810
- 34 van der Westhuysen AJ, Zijlema M, Battjes JA (2007) Saturation-based whitecap-
35 ping dissipation in SWAN for deep and shallow water. *Coastal Eng* 54:151–170
- 36 van der Westhuysen AJ, van Dongeren AR, Groeneweg J, van Vledder GP, Pe-
37 ters H, Gautier C, van Nieuwkoop JCC (2012) Improvement in spectral wave
38 modelling in tidal inlets seas. *J Geophys Res* 117:C00J28
- 39 Willebrand J (1975) Energy transport in a nonlinear and inhomogeneous random
40 gravity wave field. *J Fluid Mech* 70:113–126
- 41 Wingert KM (2001) Validation of operational global wave prediction models with
42 spectral buoy data. Master's thesis, Naval Postgraduate School, Monterey, CA
- 43 WISE Group (2007) Wave modelling - the state of the art. *Progress in Oceanog-*
44 *raphy* 75:603–674, DOI 10.1016/j.pocean.2007.05.005
- 45 Yanenko NN (1971) *The method of fractional steps*. Springer-Verlag
- 46 Zijlema M, van der Westhuysen AJ (2005) On convergence behaviour and numer-
47 ical accuracy in stationary swan simulations of nearshore wind wave spectra.
48 *Coastal Eng* 53:237–256, DOI 10.1016/j.coastaleng.2004.12.006
- 49
50
51
52
53
54
55
56
57
58
59
60
61
62
63
64
65

1 Zijlema M (2010) Computation of wind-wave spectra in coastal waters with SWAN
2 on unstructured grids. Coastal Eng 57:267–277
3
4
5
6
7
8
9
10
11
12
13
14
15
16
17
18
19
20
21
22
23
24
25
26
27
28
29
30
31
32
33
34
35
36
37
38
39
40
41
42
43
44
45
46
47
48
49
50
51
52
53
54
55
56
57
58
59
60
61
62
63
64
65